International Journal of Pressure Vessels and Piping 101 (2013) 37–44

Contents lists available at SciVerse ScienceDirect

International Journal of Pressure Vessels and Piping

journal homepage: www.elsevier.com/locate/ijpvp

Numerical investigation on weld residual stresses in tube to tube sheet joint of a heat exchanger

Shugen Xu [a,b,*], Weiqiang Wang [c]

[a] College of Chemical Engineering, China University of Petroleum (Huadong), Qingdao 266555, China
[b] State Key Laboratory of Heavy Oil Processing, China University of Petroleum (Huadong), Qingdao 266555, China
[c] School of Mechanical Engineering, Shandong University, Jinan 250061, China

ARTICLE INFO

Article history:
Received 15 July 2012
Received in revised form
7 October 2012
Accepted 10 October 2012

Keywords:
Finite element analysis
Residual stresses
Tube to tube sheet weld

ABSTRACT

Crack development in weld of the tube to tube sheet region of heat exchanger is a common problem. The residual stresses associated with welding can play a major role in this situation. In this paper, the Finite Element Method (FEM) is used to predict the residual stresses in a tube to tube sheet weld. The effect of heat input, preheating temperature, and gap between tube and tube hole on residual stresses was also investigated by numerical simulation. The peak Mises residual stress occurs in the base metal near the interface between surface welding layer and base metal. The heat input has little effect on the residual stresses. The maximum residual stress is determined by the yield strength rather than heat input. With the preheating temperature increasing, the peak hoop stresses are decreased. With the gap between tube and tube hole increasing, the residual stresses are increased.

1. Introduction

The shell-tube heat exchanger is widely used in petroleum, chemical, medicine industries. The tube to tube sheet joint is a critical element of shell-tube heat exchangers. It separates the two fluids and thus its strength has a direct effect on the safety of the process plant. This joint is made by either expansion, welding or a combination of the two processes [1]. Sometimes, the tube is made of austenitic stainless steel for anti-corrosion. The tube sheet with surface welding consisting of a thin layer of austenitic stainless steel onto a lower cost, thicker base metal, has been widely used in construction of corrosion resistant equipment. It not only has good resistance to corrosion but also can meet the strength requirement [2].

The interfaces between tube and tube sheet are particularly difficult to test, because of high temperature and large temperature gradients, as well as the complicate geometry [3]. Crack development in weld of the tube to tube sheet region of heat exchanger is a common problem. Such crack is propagated by stress corrosion cracking or thermal fatigue, or localized corrosion [4]. The local stress levels, arising from a combination of the applied loading, as well as thermal and residual stresses, contribute to the failure scenario. The SCC of austenitic stainless steels may occur when an alloy is simultaneously subject to the tensile stress and a specific corrosive medium. The residual stresses associated with welding of tube to tube sheet can play a major role in this situation [5]. Thus, in addition to paying more attention to material and environment, a good prediction and an efficient evaluation of the welding residual stress are necessary [6].

In general, welding residual stress field depends on several main factors including material properties, structural dimensions and external constraint condition, welding process parameters such as heat input, number of weld pass, welding sequence, preheating temperature and inter-pass temperature. The approaches to the welding residual stress are including experimental methods, numerical methods, and theoretical methods. Experimental methods, such as X-ray [7], hole-drilling [8], and neutron diffraction [9] are used to measure the welding residual stress in engineering. With the development of computer technology, FEM has been confirmed to be a useful and powerful numerical analysis tool to predict the welding residual stress [10–12]. It can be employed to simulate welding temperature field, welding residual stress field and welding deformation. The application of FEM is more and more popular to predict residual stresses in welded components for assessment purposes [13].

In the past, a number of FEM models [14–16] have been proposed and employed to predict welding residuals stress in

* Corresponding author. College of Chemical Engineering, China University of Petroleum (Huadong), Qingdao 266555, China. Tel.: +86 (0)532 86983482; fax: +86 (0)532 86983480.
E-mail address: xsg123@163.com (S. Xu).

0308-0161/$ – see front matter © 2012 Elsevier Ltd. All rights reserved.
http://dx.doi.org/10.1016/j.ijpvp.2012.10.004

welded structures. Brickstad et al. [17] employed 2-D axi-symmetric models to simulate a series of multi-pass circumferential butt-welds of stainless steel pipe in a non-linear thermo-mechanical FE analysis. Jiang developed a sequential coupling finite element procedure to predict residual stresses in a repair weld in a stainless steel clad plate. The effects of welding heat input and layer number [15], repair width [18], and repair length [19] on residual stresses have been discussed. Soanes et al. [20] simulated welding residual stress at a repair in steam header to tube plate weld using a 2-D axi-symmetric model. Deng [21] have compared the simulated results of both the temperature field and the welding residual stress field with experimental measurements for SUS304 stainless steel pipe. The research shows that a 2-D axi-symmetric model can also give a reasonable prediction for both the temperature field and the residual stress field in stainless steel pipe except for the welding start–finish location.

The strength, including thermal stress, mechanical stress, and welding residual stress of tube to tube sheet has received a lot of attention in recent years. Tait et al. [22] studied an experimental method to obtain the residual stresses in tube to tube sheet welds of industrial boilers. Meraha et al. [23] investigated the effect of initial radial clearance and material strain hardening on the strength of the expanded tube to tube sheet joint by using the FEM. But it is not clear the residual stress distribution in weld and Heat Affect Zone (HAZ) of tube to tube sheet joint with double pass welding. It is also not clear whether or not the preheating temperature, gaps between tube and tube hole, and heat input has effect on residual stress and it is discussed in this paper, aiming to provide a reference for optimizing the tube to tube sheet weld for the heat exchanger.

In this paper, the FEM was used to predict the residual stresses in a tube to tube sheet weld. The axi-symmetric thermal and mechanical model were established and validated by the experimental study in the literature. The effect of heat input, preheating temperature, and gap between tube and tube hole on residual stresses was also investigated by numerical simulation.

2. FE analysis of the welding residual stress

A sequential coupling thermal–structural analysis program is developed to calculate the welding temperature and residual stress by FE software ABAQUS. The thermal analysis is carried out to obtain the welding temperature history firstly, and then the temperature results are applied incrementally to the structural model to calculate the residual stress.

2.1. Geometrical model and meshing

The geometrical model of the weld of a tube to tube sheet is shown in Fig. 1. The tube sheet is a low alloy steel with surface welding layer of austenitic stainless steel. The thickness of base metal and surface welding layer metal are 230 mm and 6 mm, respectively. The tube size is $\Phi 35 \times 6.5$ mm. The weld geometry is shown in Fig. 1, and the gap between the tube and tube hole is 0.2 mm. For the calculation convenient, a part of the tube sheet is selected for the FE analysis. Although the real welding is a 3-D procedure, it is often considered sufficient to represent a circumferential weld with an axi-symmetric FE model [2,20,21]. 2-D simulations are much faster and easier to perform. Therefore, the methodology described here is based on an axi-symmetric model. A 2-D axi-symmetric model is established and the FE meshing is shown in Fig. 2. In total, 4024 nodes and 3800 elements are meshed. The welding of the tube to tube sheet containing double weld passes, as shown in Fig. 2.

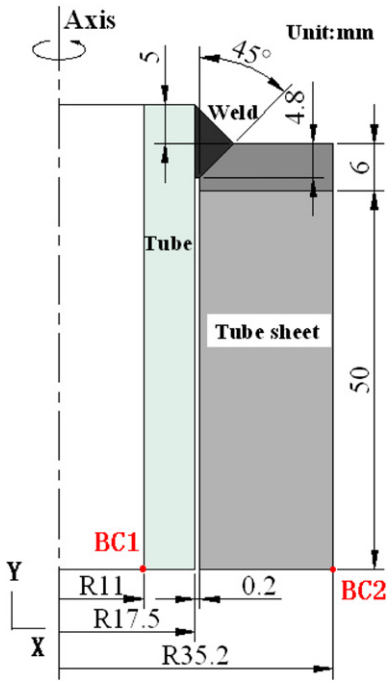

Fig. 1. The geometrical model of tube to tube sheet weld.

2.2. Material properties

The base metal of tube sheet is low alloy steel Q345R, which is a Chinese grade. The material of surface welding metal is austenitic stainless steel 1Cr18Ni9, a Chinese steel grade, which is equivalent to Type 304, and used for the requirements of corrosion resistance. The heat exchanger tube is made of 1Cr18Ni9 austenitic stainless steel. The weld metal is assumed to have the same material properties as 1Cr18Ni9 steel. The chemical compositions are listed in Table 1 [2,24]. For thermal and mechanical analysis, temperature-dependent thermo-physical and mechanical properties of the materials are incorporated, as listed in Table 2 [19].

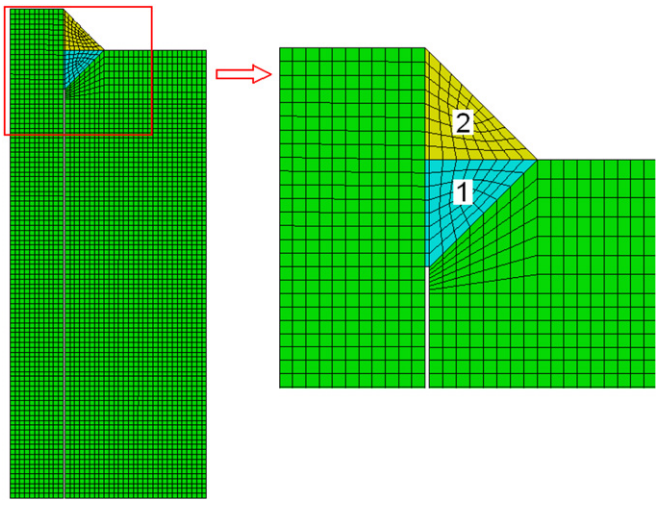

Fig. 2. FE mesh of the model.

Table 1
Chemical composition (in wt.%).

Composition	C	Si	Mn	S	P	Cr	Ni
1Cr18Ni9	0.06	0.92	0.96	0.004	0.026	18.26	9.78
Q345R	0.17	0.40	1.42	0.020	0.018	–	–

Table 2
Material properties for 1Cr18Ni9 and Q345R steel.

Temperature (°C)	20	200	400	600	800
Material properties for 1Cr18Ni9 stainless steel					
Young's modulus (GPa)	199	180	166	150	125
Yield strength (MPa)	206	153	108	82	69
Poisson's ratio	0.28	0.28	0.28	0.28	0.28
Density (kg/m^3)	8010	7931	7840	7755	7667
Thermal expansion (1/°C × 10^{-6})	16.0	17.2	18.2	18.6	19.5
Thermal conductivity (W/m °C)	15.26	17.6	20.2	22.8	25.4
Specific heat (J/kg °C)	500	544.3	582	634	686
Material properties for Q345R steel					
Young's modulus (GPa)	200	183	160	150	125
Yield strength (MPa)	345	310	280	210	160
Poisson's ratio	0.3	0.3	0.3	0.3	0.3
Density (kg/m^3)	7850	7840	7830	7820	7810
Thermal expansion (1/°C × 10^{-6})	14.0	14.2	16.0	16.6	18
Thermal conductivity (W/m °C)	53.17	47.73	39.57	36.01	33
Specific heat (J/kg °C)	461	523	607	678	700

2.3. Thermal analysis

The simulation of weld metal deposition is achieved by "Element birth and death" technology. To achieve the "element death" effect, the ABAQUS program does not actually remove "killed" elements. Instead, it deactivates them by multiplying their stiffness (or conductivity, or other analogous quantity) by a severe reduction factor. Before welding, the weld metal elements are killed. Once the welding starts, the welded pass is alive and heated, then it is cooled down until the next weld pass cycle begins.

The distributed heat flux, DFLUX, is given by

$$\mathrm{DFLUX} = \frac{UI\eta}{V} \tag{1}$$

where U is the voltage, I is the current, η is the arc efficiency and V is the weld pass volume. The weld pass volume V, which is a 3-D parameter, is related to the duration t that is equal to the time taken by the weld electrode to move around volume V, causing it to

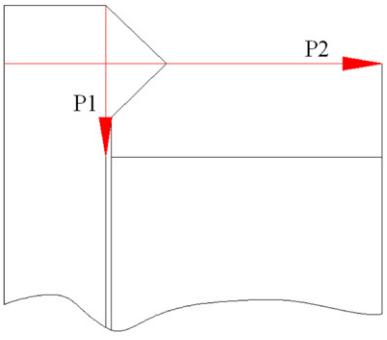

Fig. 3. Location of reference paths.

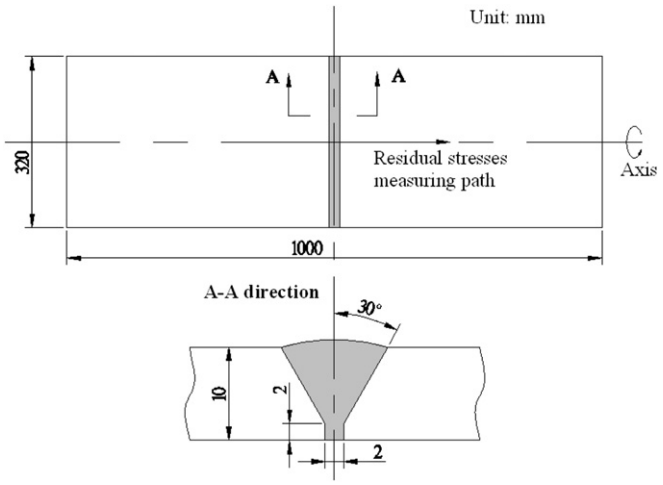

Fig. 4. Geometrical model of weld to verify the FE analysis.

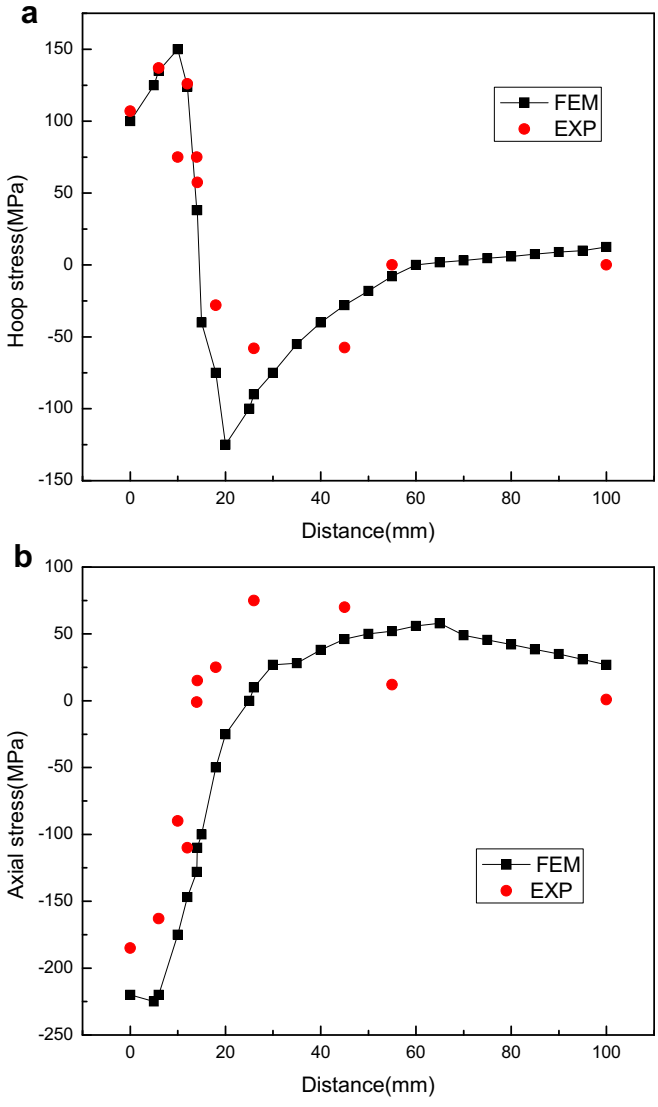

Fig. 5. A comparison of the hoop (a) and axial residual stress (b) by our FEM and Sattari-Far's experiment.

melt, as it travels around the circumference at speed v. The net line energy is given by

$$Q = \frac{UI\eta}{v} \tag{2}$$

According to Eqs. (1) and (2), the distributed heat flux is given by

$$\mathrm{DFLUX} = \frac{Qv}{V} \tag{3}$$

The voltage, current and speed used in the calculation is 18 V, 90 A and 3 mm/s. The value of V can only be estimated, since it relates to the effective volume of weld material directly influenced by the heat generation in the axi-symmetric simulation. As a guideline, a fraction of the circumference equal to 1/16–1/2 of a radian can be used to estimate V [25]. In this simulation, the value 1/16 is used.

As for the boundary conditions during the thermal analysis, convection and radiation are both taken into consideration and their combined effect is represented in the following two equations for the temperature-dependent heat transfer coefficient, h [25]:

$$h = \begin{cases} 0.0668T & \text{when } 0 \le T \le 500\ ^\circ\mathrm{C} \\ 0.231T - 82.1 & \text{when } T > 500\ ^\circ\mathrm{C} \end{cases} \tag{4}$$

2.4. Structural analysis

The residual stress is calculated by using the temperature distribution obtained from thermal analysis as input data. Element birth and death technique has also been used in stress analysis. The material properties relevant to residual stress are Young's modulus, yield strength, Poisson's ratio, and the coefficient of thermal expansion. During the welding process, because solid-state phase transformation does not occur in the stainless base metal and the weld metal, the total strain can be decomposed into three components as follows:

$$\varepsilon = \varepsilon^e + \varepsilon^p + \varepsilon^t \tag{5}$$

where ε^e, ε^p, and ε^t are elastic strain, plastic strain and thermal strain, respectively. Elastic strain is modeled using the isotropic Hooke's law with temperature-dependent Young's modulus and Poisson's ratio. The thermal strain is calculated using temperature-dependent coefficient of thermal expansion. For the plastic strain, a plastic model is employed with Von Mises yield criterion, temperature-dependent mechanical properties and linear kinematic hardening model. Kinematic hardening is considered because material points undergo both loading and unloading in the welding process, which has been widely used in the welding residual stress simulation.

During the structural analysis, boundary conditions should be applied to prevent the rigid body motion. Because of the axi-symmetry of the FE model, BC1 is constrained in X-direction. BC2 is constrained in Y-direction.

In order to analyze the results, 2 paths named P1 and P2 are defined as shown in Fig. 3. P1 is along the outer surface of the tube, P2 is through the whole thickness of tube, and along the tube sheet surface.

3. Verification of the FE modeling

To verify the result of FE simulation, a FE model with same geometrical, material and welding parameters with those used in the Sattari-Far's paper is generated, as shown in Fig. 4 [26].

A 2-D axi-symmetric of the pipe welding model is established. The material of the pipe is AISI-304 stainless steel. The temperature-dependent mechanical and thermal properties of material are as the

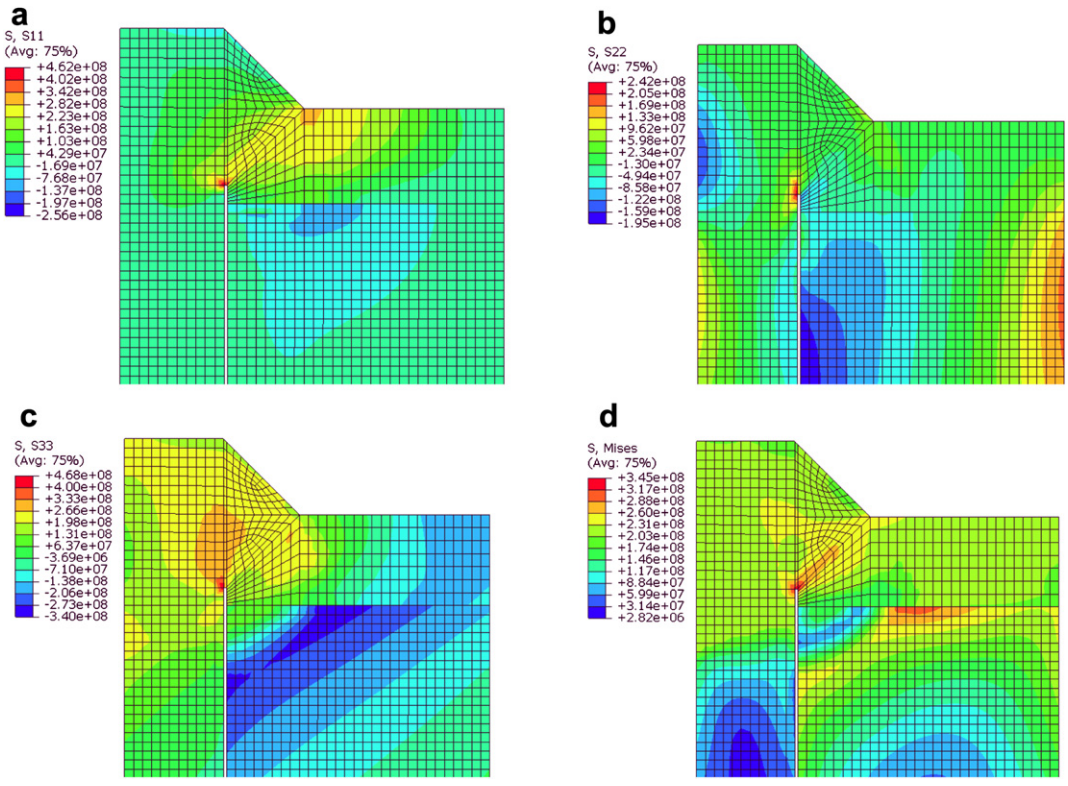

Fig. 6. The residual stress contour: radial stress (a), axial stress (b), hoop stress (c) and Von Mises stress (d).

same as in the literature [26]. The distributed heat flux and element birth and death technique is used for the thermal analysis. The kinematic hardening model is considered for the structural analysis.

The hoop and axial stresses on the outside surface along the axial direction obtained from the FE by analysis and the experimental measurements by Sattari-Far are shown in Fig. 5. It is observed that the predicted results from the FE analysis are in relatively good agreement with the experimental measurements. Therefore, the FE program developed here can be used for residual stress analysis in the tube to tube sheet welding in this paper.

4. Results and discussion

4.1. Residual stress distribution contour

The stress contours of radial stress, axial stress and hoop stress is shown in Fig. 6. The peak stresses of radial stress, axial stress and hoop stress are 462, 242 and 468 MPa. The peak stresses of radial stress, axial stress and hoop stress are located on the weld root zone as shown in Fig. 6. The peak Mises stress is located on the base metal near the interface between base metal and surface welding layer. It also can be seen that the stress in surface welding layer and base metal is not continuous. This is because the yield strength of base metal is larger than surface welding layer. The mismatching of yield strength between base metal and surface welding layer caused an unbalanced distribution of residual stresses.

Fig. 7 shows the stress distribution along the reference path P1 and reference path P2. The reference path P1 can be divided into two parts: weld edge and HAZ. All the stress components have the same trend along P1, as shown in Fig. 7(a). Along P1, all the stress increases firstly, and then decrease and keep low level in the HAZ.

The reference path P2 can be divided into three parts: the wall of tube, WCL and HAZ. Along the wall of tube, all the stress increases. The radial stress and hoop stress are tensile stress, and the axial stress is compressive stress. Along the WCL, the radial stress increases and reaches to its peak value. The hoop stress decreases. The axial stress is fairly low; it decreases firstly, and then increases to its peak value. Along the HAZ, which is the outer surface of tube sheet, all the stresses decrease.

4.2. Effect of weld heat input on residual stress

In order to obtain the effect of gap between tube and tube sheet on residual stress, keeping the rest of the welding parameters constant, three models with the heat input of 3.38 kJ/cm, 4.32 kJ/cm, and 5.76 kJ/cm were established to discuss the influence of heat input.

Fig. 8 shows the effect of heat input on the residual stresses along P1. It is shown that the three models have almost the same stress distribution, but all the peak residual stresses are increased with the heat input increasing. Fig. 9 shows the effect of heat input on residual stress along P2. It is also observed that the heat input did not affect the stress distribution law. The stresses distributions are almost the same. Both the peak residual radial and hoop stresses are increased with the heat input increasing, but the axial stress is decreased with the heat input increasing.

4.3. Effect of preheating temperature on residual stress

In order to study the effect of preheating temperature on residual stress, keeping the rest of the welding parameters constant, three models with a preheating temperature of 50 °C, 100 °C, and 150 °C were developed to discuss the influence of preheating temperature. Fig. 10 shows the radial, axial and hoop stress with different preheating temperature, versus distance along the P1. It is shown that the peak stresses are decreased with preheating temperature increase, which is located on the weld root zone. For example, when the preheating temperature is 50 °C, the maximum hoop stress is 480 MPa. When the preheating temperature increases to 150 °C, the maximum hoop stress is 453 MPa. In the other zone, the stresses have a little variation. Based on this result, it can be confirmed that the preheating temperature on peak residual stress is significant, and increasing the preheating temperature can decrease the peak residual stress in the structure.

4.4. Effect of gap between tube and tube hole on residual stress

In order to investigate the effect of gap between tube and tube hole on residual stress, keeping the rest of the welding parameters constant, three models with a gap of 0.1 mm, 0.15 mm, and 0.2 mm were established to discuss the influence of gap between tube and tube hole. It can be seen that the gap has an effect on residual stress, as shown in Fig. 11. The distributions of all the residual radial stresses have a little difference. The residual axial and hoop stresses are increased with the gap between tube and tube hole increasing. Based on this result, it can be confirmed that the decreasing the gap can decrease the residual stress in the structure.

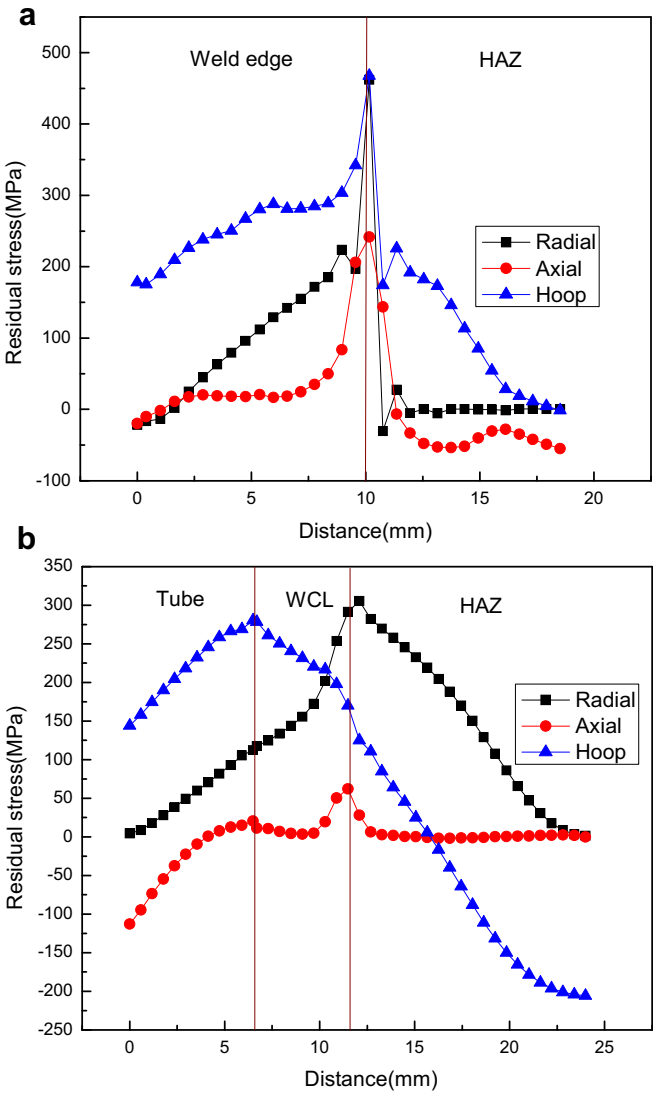

Fig. 7. Residual stress distribution along P1 (a) and P2 (b).

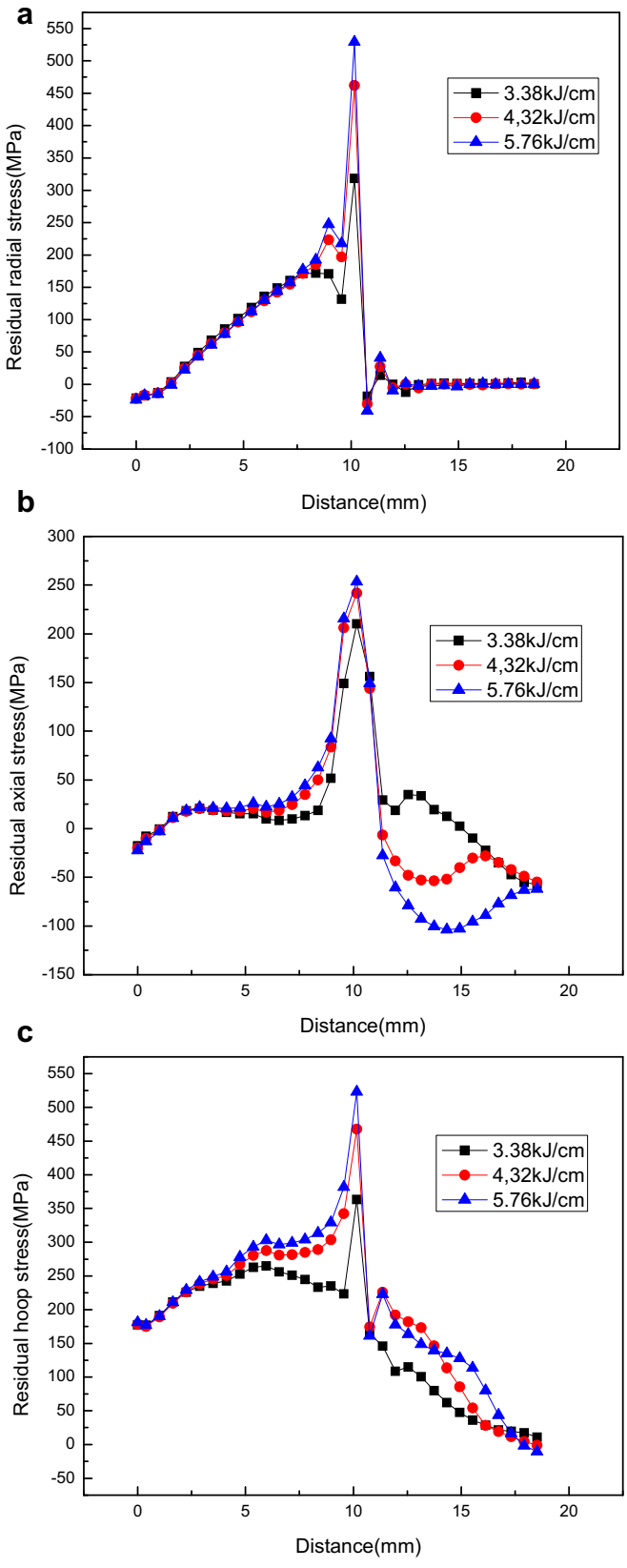

Fig. 8. Effect of heat input on residual stress along P1.

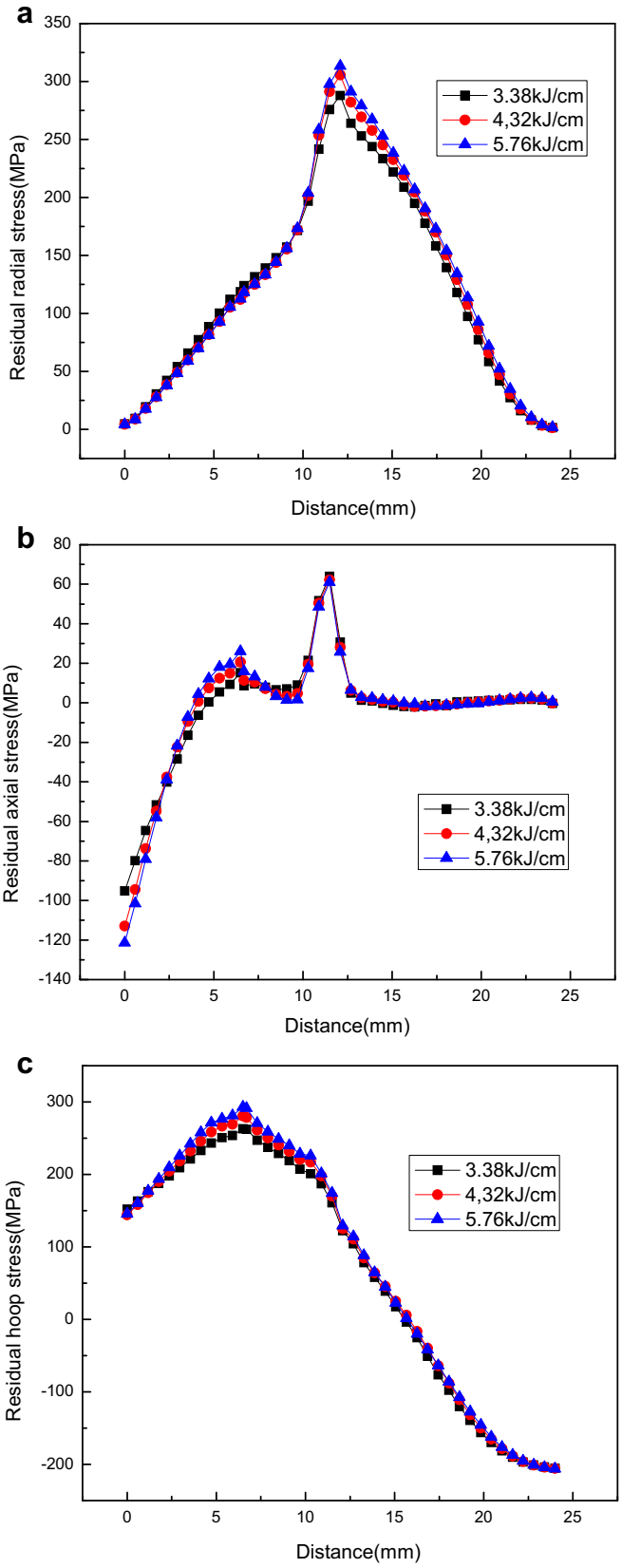

Fig. 9. Effect of heat input on residual stress along P2.

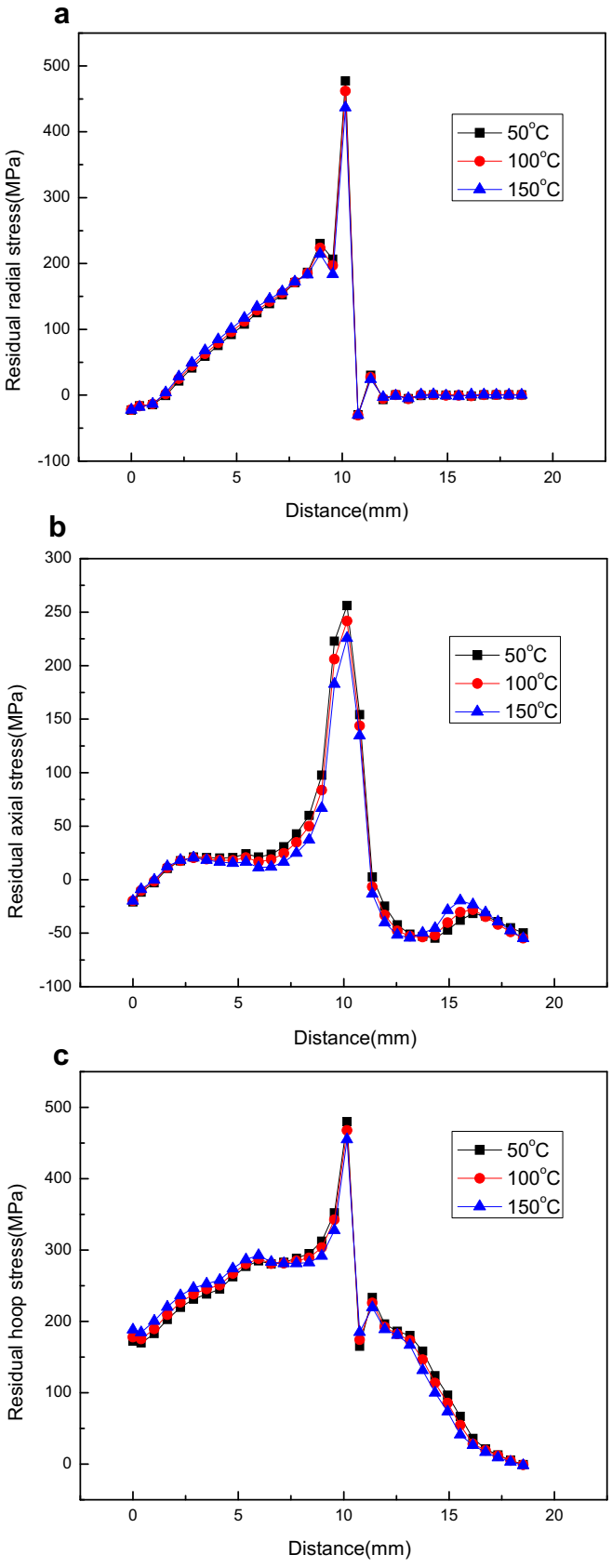

Fig. 10. Effect of preheating temperature on residual stress along P1. Radial stress (a), axial stress (b), and hoop stress (c).

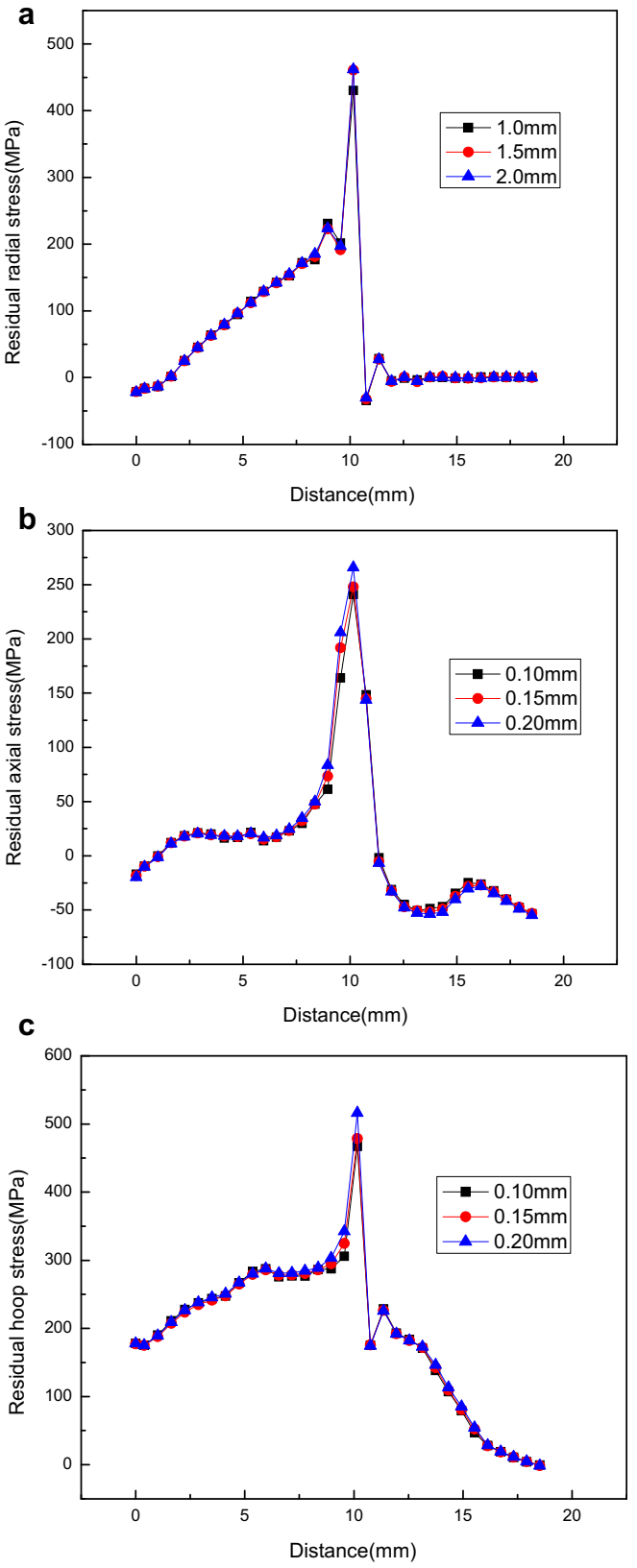

Fig. 11. Effect of gap on residual stress along P1. Radial stress (a), axial stress (b), and hoop stress (c).

5. Conclusions

Residual stress in tube to tube sheet welding of a heat exchanger is numerically investigated with an axi-symmetric FE model. The detailed two pass simulation with element birth is performed to demonstrate the evolution of the residual stress. The main conclusions can be summarized as follows:

(1) Due to the material mismatching between surface welding and base metal, a discontinuous stress distribution has been generated across the interface between surface welding and base metals. The peak residual Mises stress occurs in the base metal near the interface between surface welding layer and base metals.
(2) The heat input, welding preheating temperature, gap between tube and tube hole have effect on residual stresses. They have no significant effect on residual stress distribution law, but change the values of residual stresses.
(3) The heat input has a little effect on the residual stresses. The maximum residual stress is determined by the yield strength rather than heat input. With the preheating temperature increase, the peak residual stresses are decreased. With the gap between tube to tube sheet increases, the peak residual stresses are increased.

However, in this paper, a single tube is selected for the analysis of weld temperature and residual stress, and welding effect of other tubes around it is ignored. The 3-D welding model of multi-tubes should be considered in future research.

Acknowledgment

This research work was financial supported by the Fundamental Research Funds for the Central Universities (27R1204022A).

References

[1] Merah N, Al-Zayer A. Finite element evaluation of clearance effect on tube-to-tube sheet joint strength. Int J Pres Ves Pip 2003;80(12):879–85.
[2] Xu Shugen, WANG Weiqiang, Liu Huadong. The stress corrosion cracking of austenitic stainless steel heat exchange tubes—three cases study, vol. 5. ASME, Pressure Vessels and Piping Division (Publication) PVP; 2010. p. 335–43.
[3] Kim Soon-Tae, Kim Seong-Yoon, Lee In-Sung, Park Yong-Soo, Shin Min-Chul, Kim Young-Sub. Effects of shielding gases on the microstructure and localized corrosion of tube-to-tube sheet welds of super austenitic stainless steel for seawater cooled condenser. Corros Sci 2011;53(8):2611–8.
[4] Azevedo CRF, Beneduce Neto F, Brandi SD, Tschiptschin AP. Cracking of 2.25Cr–1.0Mo steel tube/stationary tube-sheet weldment of a heat-exchanger. Eng Fail Anal 2008;15(6):695–710.
[5] Ghosh Swati, Singh Rana Vishav Preet, Kain Vivekanand, Mittal Vivek, Baveja SK. Role of residual stresses induced by industrial fabrication on stress corrosion cracking susceptibility of austenitic stainless steel. Mater Des 2011; 32(7):3823–31.
[6] Nam Jun-Young, Seo Duck-hee, Lee Sang-yun, Hwang Woong-Ki, Lee Bo-Young. The effect of residual stress on the SCC using ANSYS. Procedia Eng 2011;10:2609–14.
[7] Martins J-A, Cardoso L-P, Fraymann J-A, Button S-T. Analyses of residual stresses on stamped valves by X-ray diffraction and finite elements method. J Mater Process Tech 2006;179(1–3):30–5.
[8] Bouchard P-J, George D, Santisteban J-R, Bruno G, Dutta M, Edwards L, et al. Measurement of the residual stresses in a stainless steel pipe girth weld containing long and short repairs. Int J Pres Ves Pip 2005;82(4): 299–310.
[9] Turski M, Francis JA, Hurrell PR, Bate SK, Hiller S, Withers PJ. Effects of stop–start features on residual stresses in a multi-pass austenitic stainless steel weld. Int J Pres Ves Pip 2012;89:9–18.
[10] Jiang Wenchun, Zhang Yucai, Woo Wanchuck. Using heat sink technology to decrease residual stress in 316L stainless steel welding joint: finite element simulation. Int J Pres Ves Pip 2012;92:56–62.
[11] Kim Jong Sung, Seo Joong Hyun. A study on welding residual stress analysis of a small bore nozzle with dissimilar metal welds. Int J Pres Ves Pip 2012;90–91:69–76.
[12] Hyde TH, Luo R, Becker AA. Prediction of three-dimensional residual stresses at localised indentations in pipes. Int J Pres Ves Pip 2012;93-94:1–11.
[13] Xu LY, Cheng YF. Reliability and failure pressure prediction of various grades of pipeline steel in the presence of corrosion defects and pre-strain. Int J Pres Ves Pip 2012;89:75–84.
[14] Zain-ul-Abdein Muhammad, Nélias Daniel, Jullien Jean-François, Boitout Fréderic, Dischert Luc, Noe Xavier. Finite element analysis of metallurgical phase transformations in AA 6056-T4 and their effects upon the residual stress and distortion states of a laser welded T-joint. Int J Pres Ves Pip 2011;88(1):45–56.
[15] Jiang Wenchun, Liu Zibai, Gong JM, Tu ST. Numerical simulation to study the effect of repair width on residual stresses of a stainless steel clad plate. Int J Pres Ves Pip 2010;88(8):457–63.
[16] Akbari D, Sattari-Far I. Effect of the welding heat input on residual stresses in butt-welds of dissimilar pipe joints. Int J Pres Ves Pip 2009; 86(11):769–76.
[17] Brickstad B, Josefson BL. A parametric study of residual stresses in multi-pass butt-welded stainless steel pipes. Int J Pres Ves Pip 1998;75:11–25.
[18] Jiang WC, Wang BY, Gong JM, Tu ST. Finite element analysis of the effect of welding heat input and layer number on residual stress in repair welds for a stainless steel clad plate. Mater Des 2011;32:2851–7.
[19] Jiang Wenchun, Xua XP, Gong JM, Tu ST. Influence of repair length on residual stress in the repair weld of a clad plate. Nucl Eng Des 2012;246:211–9.
[20] Soanes TPT, Bell W, Vibert AJ. Optimizing residual stresses at a repair in a steam header to tube plate weld. Int J Pres Ves Pip 2005;82(4):311–8.
[21] Deng Dean, Murakawa Hidekazu. Numerical simulation of temperature field and residual stress in multi-pass welds in stainless steel pipe and comparison with experimental measurements. Comp Mater Sci 2006;37(3):269–77.
[22] Tait RB, Press J. An experimental study of the residual stresses, and their alleviation, in tube to tube-sheet welds of industrial boilers. Eng Fail Anal 2001;8(1):15–27.
[23] Meraha N, Al-Zayerb A, Shuaiba A, Arif A. Finite element evaluation of clearance effect on tube-to-tube sheet joint strength. Int J Pres Ves Pip 2003; 80(12):879–85.
[24] Xu Shugen, Wang Weiqiang, Liu Huadong, Zhang Anjun, Tang Jun. Catastrophic explosion of a multilayered urea reactor. Ammonia Plant Saf Relat Facil 2008;49:375–86.
[25] Yaghi A, Hyde TH, Becker AA, Sun W, Williams JA. Residual stress simulation in thin and thick-walled stainless steel pipe welds including pipe diameter effects. Int J Pres Ves Pip 2006;83(11–12):864–74.
[26] Sattari-Far I, Farahani MR. Effect of the weld groove shape and pass number on residual stresses in butt-welded pipes. Int J Pres Ves Pip 2009;86(11):723–31.